WILEY

Protein resonance assignment by BSH-CP-based 3D solid-state NMR experiments: A practical guide

Jutta Hoffmann[1] | Julia Ruta[1] | Chaowei Shi[1] | Kitty Hendriks[1] (ID) |
Veniamin Chevelkov[1] | W. Trent Franks[2] | Hartmut Oschkinat[2] | Karin Giller[3] |
Stefan Becker[3] | Adam Lange[1,4] (ID)

[1] Department of Molecular Biophysics, Leibniz-Forschungsinstitut für Molekulare Pharmakologie, Berlin, Germany

[2] Department of NMR-supported Structural Biology, Leibniz-Forschungsinstitut für Molekulare Pharmakologie, Berlin, Germany

[3] Department of NMR-based Structural Biology, Max Planck Institute for Biophysical Chemistry, Göttingen, Germany

[4] Institut für Biologie, Humboldt-Universität zu Berlin, Berlin, Germany

Correspondence
Adam Lange, Department of Molecular Biophysics, Leibniz-Forschungsinstitut für Molekulare Pharmakologie, Berlin 13125, Germany.
Email: alange@fmp-berlin.de

Funding information
European Research Council; Max Planck Society; Leibniz-Forschungsinstitut für Molekulare Pharmakologie

Abstract

Solid-state NMR (ssNMR) spectroscopy has evolved into a powerful method to obtain structural information and to study the dynamics of proteins at atomic resolution and under physiological conditions. The method is especially well suited to investigate insoluble and noncrystalline proteins that cannot be investigated easily by X-ray crystallography or solution NMR. To allow for detailed analysis of ssNMR data, the assignment of resonances to the protein atoms is essential. For this purpose, a set of three-dimensional (3D) spectra needs to be acquired. Band-selective homo-nuclear cross-polarization (BSH-CP) is an effective method for magnetization transfer between carbonyl carbon (CO) and alpha carbon (CA) atoms, which is an important transfer step in multidimensional ssNMR experiments. This tutorial describes the detailed procedure for the chemical shift assignment of the backbone atoms of ^{13}C–^{15}N-labeled proteins by BSH-CP-based ^{13}C-detected ssNMR experiments. A set of six 3D experiments is used for unambiguous assignment of the protein backbone as well as certain side-chain resonances. The tutorial especially addresses scientists with little experience in the field of ssNMR and provides all the necessary information for protein assignment in an efficient, time-saving approach.

KEYWORDS
BSH-CP, magic-angle spinning, protein NMR, resonance assignment, solid-state NMR

1 | INTRODUCTION

To obtain information about the three-dimensional structure of a protein and its dynamics, many different techniques can nowadays be applied. When it comes to insoluble proteins,[1–3] for example, oligomeric assemblies,[4] bacterial structures,[5] amyloid fibrils,[6,7] or membrane proteins,[8–11] the application of protein X-ray crystallography and solution NMR spectroscopy can be very difficult or even impossible. These proteins crystallize only very reluctantly, if at all, and are not easily kept in solution either. For the structural investigation

---

Jutta Hoffmann and Julia Ruta contributed equally to this work.

of these kinds of proteins, cryo-electron microscopy and solid-state NMR (ssNMR) can serve as useful methods where neither crystal formation nor solubilization are required. In contrast to cryo-electron microscopy, where samples are studied in the frozen state, ssNMR allows for measurements in a wide temperature range (−200°C to 120°C) and under different sample conditions. Membrane proteins can be observed in a lipid environment, and amyloid proteins can be observed in the fibrillar state mimicking natural conditions and therefore valorizing the structural and dynamic information thus obtained.

Key to this information is the ability to assign the resonances in the NMR spectra to the atoms in the protein, in a process that is well established for ^{13}C–^{15}N-labeled samples.[12] The assignment should preferably result in a complete list of the protein atoms and their corresponding chemical shifts.

For such an assignment, an isotope-labeled sample of the protein needs to be produced and subjected to proton-detected or carbon-detected ssNMR experiments. A detailed guide regarding practical considerations in solid-state NMR[13] and a protocol for the backbone assignment of perdeuterated proteins using proton detection[14] have recently been published by our group. The protocol described here is meant as a guide for backbone assignment of proteins using carbon detection ssNMR, supplying information complementary to the two publications mentioned above.

The acronyms listed in Table 1 will be used in this tutorial to refer to recoupling and decoupling schemes.

TABLE 1 Meaning of the acronyms used in this tutorial

Acronym	Meaning
BSH-CP	Band-selective homo-nuclear cross-polarization
CP	Cross polarization
CW	Continuous wave decoupling
DARR/RAD	Dipolar-assisted rotational resonance/RF-assisted diffusion
DREAM	Dipolar recoupling enhanced by amplitude modulation
MIRROR	Mixed rotational and rotary-resonance condition
PDSD	Proton-driven spin diffusion
SPECIFIC-CP[15]	Spectrally induced filtering in combination with cross-polarization
SPINAL-64	Small phase incremental alternation with 64 steps

2 | BSH-CP

To obtain information about interresidual correlations and thus achieve the chemical shift assignment, a set of multidimensional hetero-nuclear correlation experiments (such as (H)NCO, (H)NCA, (H)NCOCA, and (H)NCACB) is needed. An important building block in the pulse scheme of these multidimensional experiments is the CO–CA magnetization transfer step.

At strong external magnetic fields of about 700 to 900 MHz of proton Larmor frequency, moderate magic angle spinning (MAS) rates of around 20 kHz are favorable for efficient suppression of the chemical shift anisotropy in order to increase sensitivity and resolution. Under these conditions, the more commonly used recoupling techniques such as proton-driven spin diffusion (PDSD),[16] DARR/RAD[17,18], MIRROR,[19] and DREAM[20] are less powerful or not applicable for magnetization transfer between CO and CA spins. The second-order recoupling techniques like PDSD, DARR, and MIRROR are less efficient because of increased Zeeman energy difference between CA and CO spins at higher external magnetic fields and because of stronger suppression of dipolar couplings by faster sample rotation.

The DREAM transfer requires the spinning rate notably exceeding the isotropic chemical shift difference between CO and CA spins.[20] This condition is not achievable when employing 3.2-mm probe heads at high magnetic fields of about 20 T. In case of the more conventional, second-order recoupling methods (PDSD/DARR/MIRROR), the transfer is nonselective and unwanted magnetization exchanges occur that deteriorate resolution, sensitivity, and clarity of spectra. Band-selective homo-nuclear cross-polarization (BSH-CP) and DREAM function via a first-order recoupling mechanism. Thus, the dipolar truncation prevents undesired sequential and long-range magnetization transfers. Also, in most cases, first-order recoupling techniques are preferable to second-order schemes, because they yield a larger recoupling scaling factor. However, much higher spinning speeds than 20 kHz are required for DREAM transfer between CO and CA at external magnetic fields of about 20 T. Here, BSH-CP is preferable in terms of applicability, when using 3.2-mm rotors.

For successful magnetization transfer via BSH-CP, the Hartmann–Hahn condition (Equation 1) needs to be fulfilled in that the sum or difference of the effective fields on CO ($\omega_{eff,CO}$) and CA ($\omega_{eff,CA}$) equals an integer multiple ($n = 1$ or 2) of the MAS rate (ω_r).

$$|\omega_{eff,CO} \pm \omega_{eff,CA}| = n \times \omega_r. \qquad (1)$$

The effective field ($\omega_{eff,X}$) for a nucleus is determined by the applied radiofrequency (RF) field (ω_{rf}) and the isotropic chemical shift offset Ω of the nucleus from the carrier frequency, as represented by Equation (2).

$$\omega_{eff,X} = \sqrt{(\omega_{rf}{}^2 + \Omega^2)}. \tag{2}$$

For BSH-CP, it is recommended to set the carrier frequency to the center of the CA region. Thus, negative effects of the relatively large chemical shift dispersion of the CA resonances can be minimized.[21,22] The BSH-CP RF field equals the effective field applied on CA (Equation 3):

$$\omega_{rf} = \omega_{eff,CA}. \tag{3}$$

At the considered experimental conditions, double-quantum (DQ) recoupling occurs when the sum of the effective fields acting on CO and CA is equal to two ($n = 2$) times the spinning rate, whereas zero-quantum (ZQ) recoupling takes place when the difference between two RF fields results to one ($n = 1$).[21] Previous theoretical analysis shows that the recoupling scaling factor for the DQ transfer is more than two times larger than the one for the ZQ transfer, which makes the DQ condition significantly better. Equation (1) shows that the RF field required for the DQ recoupling is approximately 2.5 times stronger than the RF field necessary for the ZQ recoupling. Higher RF fields are also more preferable, because they minimize negative consequences of isotropic chemical shift variation and anisotropic chemical shifts more.

Setting the offset of the BSH-CP pulse to CA generates an effective field on CA, which equals the applied BSH-CP RF field, and also a dissimilar effective field on CO by virtue of the chemical shift difference (Ω). Thus, a trim pulse on CO needs to be applied directly preceding or following the BSH-CP pulse. A trim pulse after the BSH-CP transfer is required when transferring magnetization from CA to CO, to flip the CO magnetization that builds up along the CO effective field during BSH-CP into the x–y plane for detection of maximal signal (Figure 1).
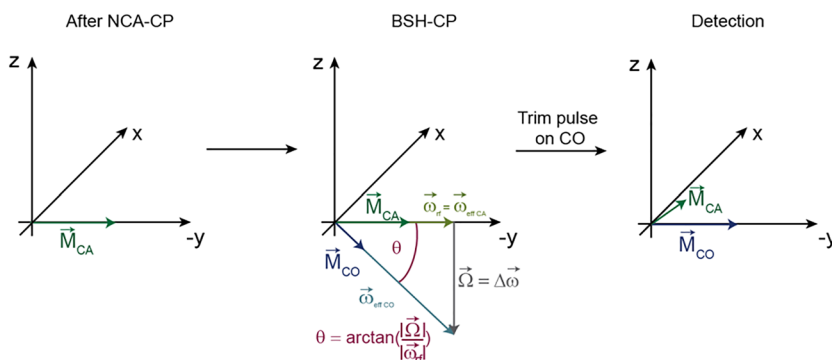
To transfer magnetization from CO to CA, a trim pulse preceding the BSH-CP pulse is necessary. Thus, CO magnetization (located in the x–y plane after the NC-CP) coincides with the effective field on CO during the BSH-CP pulse (Figure 2). For detailed instructions on how to calculate the BSH-CP and the CO trim pulses, see Box 2.

By making use of BSH-CP transfer steps between CO and CA, robust and efficient recoupling can be achieved in highly deuterated and protonated protein samples.[21,22] An optimal BSH-CP recoupling effect is obtained when the sum of the effective RF fields on CO and CA equals twice the MAS frequency. Under this condition, BSH-CP can yield magnetization transfer efficiencies of up to 50% for highly deuterated[21] and up to 40% for protonated proteins (as shown here).

Thanks to the higher transfer efficiency, an experiment featuring a BSH-CP transfer block can yield spectra of the same quality as other recoupling techniques, while using less scans. Depending on the sample quality, a complete set of 3D spectra for resonance assignment can be recorded within 1 week.[23]

BSH-CP-based experiments are suited for a wide range of samples and have already been successfully applied to different kinds of proteins such as membrane proteins,[24,25] amyloid fibrils,[26–28] and microcrystalline

FIGURE 1 Schematic representation of the BSH-CP step in the (H)NCACO experiment. After the NCA-CP step, the CA bulk magnetization ($\vec{M}_{CA}$) is in the x–y plane. For BSH-CP magnetization transfer from CA to CO an RF pulse is applied along −y on resonance with CA, with the resulting field ($\vec{\omega}_{rf}$) thus equaling the CA effective field ($\vec{\omega}_{eff,CA}$). During BSH-CP, CO magnetization ($\vec{M}_{CO}$) builds up along the CO effective field ($\vec{\omega}_{eff,CO}$). Because of the chemical shift difference between CA and CO (Ω), the CO effective field is not in the x–y plane but differs from it by the angle θ. A hard trim pulse is therefore applied on CO to flip the CO magnetization into the x–y plane for detection
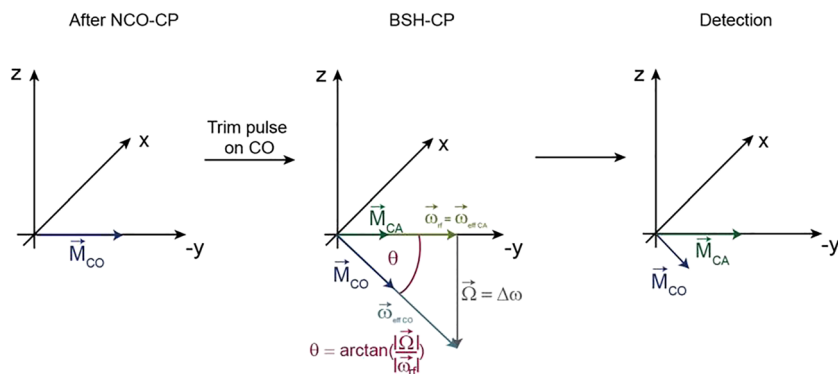
FIGURE 2 Schematic representation of the BSH-CP step in the (H)NCOCA experiment. After the NCO-CP step, the CO bulk magnetization ($\vec{M}_{CO}$) is in the x–y plane. For BSH-CP magnetization transfer from CO to CA, an RF pulse ($\vec{\omega}_{rf}$) has to be applied on resonance with CA and thus along the CA effective field ($\vec{\omega}_{eff,CA}$). Because of the chemical shift difference between CA and CO (Ω), the CO effective field is not in the x–y plane but differs from it by the angle θ. A hard trim pulse therefore has to be applied on CO beforehand to flip the CO magnetization along its effective field and fulfill the conditions for BSH-CP. During BSH-CP, CA magnetization ($\vec{M}_{CA}$) builds up in the x–y plane, in place for detection without further trim pulses required

protein samples,[29] as well as protein filaments and supramolecular assemblies.[30,31]

In order to highlight practical advantages of the technique, we compared the performance of the BSH-CP method to widely employed PDSD and MIRROR recoupling methods in NCOCX experiments. Figure 3 shows the spectra of PEG precipitated uniformly ^{13}C–^{15}N-labeled ubiquitin recorded at MAS rates of
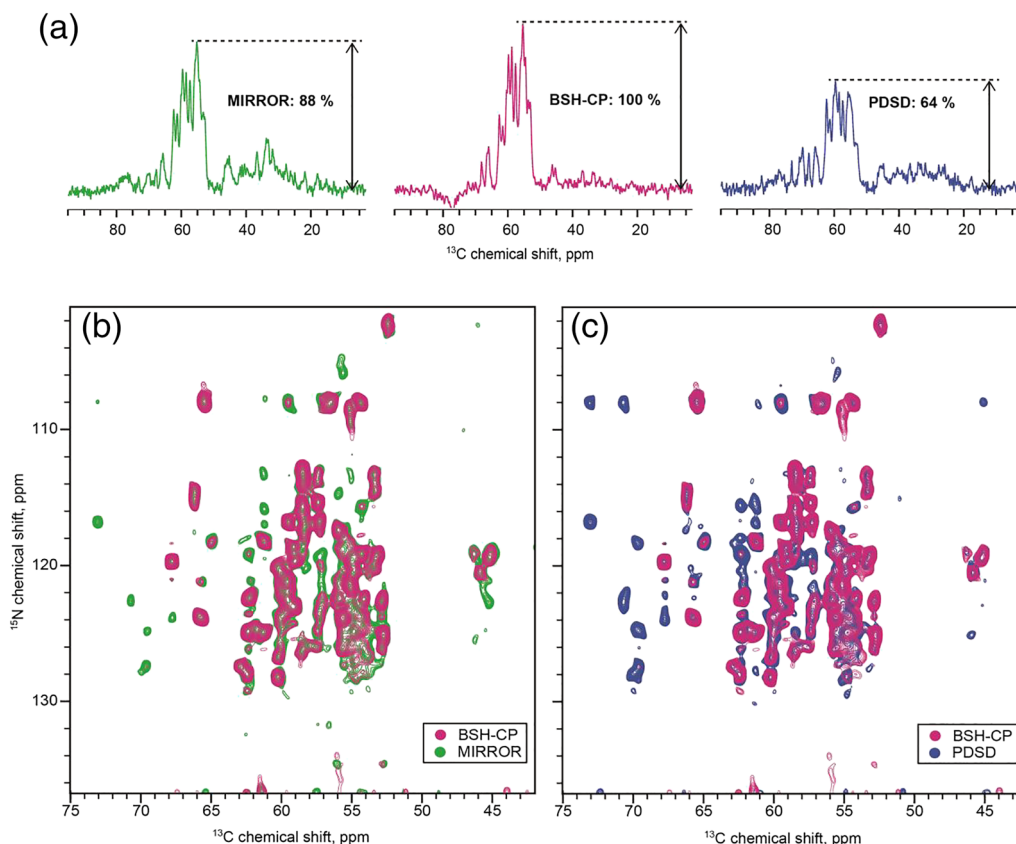
FIGURE 3 (a) 1D spectra of aliphatic regions of uniformly ^{13}C–^{15}N-labeled ubiquitin acquired by MIRROR and BSH-CP-based (H) NCOCA and PDSD-based (H)NCOCX experiments. (b, c) Comparison of 2D (H)NCA spectra obtained by BSH-CP (magenta) and MIRROR-based (H)NCOCA (green) and PDSD-based (H)NCOCX (blue) experiments on uniformly ^{13}C–^{15}N-labeled ubiquitin

21 kHz on a wide-bore instrument operating at 850 MHz of ^{1}H Larmor frequency. The CO–CA recoupling time of the BSH-CP step in the (H)NCOCA experiment was 4.4 ms with an RF pulse ramped down to 80% from an initial value of 15.1 kHz, whereas the mixing time of the PDSD was set to 100 ms. The transfer of magnetization by MIRROR was achieved in a 25 ms recoupling period with a proton RF field of 14.9 kHz that yields maximal CA signal. Figure 3a shows significant advantages of the BSH-CP recoupling. 2D (H)NCA spectra obtained by (H)NCOCX experiments employing the three different mechanisms for CO–CA magnetization transfer are represented in Figure 3b,c. Due to the nature of second-order recoupling techniques, PDSD and MIRROR-based spectra exhibit a considerable number of long range and relay correlation cross peaks. These peaks are undesirable for assignment experiments because these are not interresidual correlations between N_i and CA_{i-1} nuclei. In comparison, BSH-CP spectra do not yield such unwanted peaks, as we found in our previous detailed studies.[21–23]

This tutorial describes the procedure for the chemical shift assignment of the backbone atoms of ^{13}C–^{15}N-labeled proteins by BSH-CP-based carbon-detected ssNMR experiments, using a set of six 3D experiments that enables unambiguous assignment of the protein backbone as well as certain side-chain resonances.

3 | MATERIALS

To perform the experiments in this tutorial, a uniformly ^{13}C–^{15}N-labeled protein sample is required. For a 3.2-mm rotor, sample amounts of approximately 20 mg are necessary to fill a rotor completely (without spacers). For a 3.2-mm-thin wall rotor, which is preferable to a regular wall rotor regarding signal intensity, about 40% more sample is needed for complete filling. A small amount (spatula point) of DSS (4,4-dimethyl-4-silapentane-1-sulfonic acid) added to the sample can be used for precise chemical shift referencing.

TABLE 2 Guidance MAS frequencies and pulse radiofrequencies (ω_{rf}) for the implementation of BSH-CP-based ssNMR experiments on different spectrometers

Spectrometer (MHz)	MAS frequency (kHz)	Ideal ω_{rf} ($\omega_{eff,CA}$)
600	15	9.6 kHz
700	17.5	11.2 kHz
800	20	12.8 kHz
900	22.5	14.4 kHz

The optimum MAS spinning rate depends on the strength of the magnetic field used; guidance MAS frequencies are listed in Table 2. The cooling unit must be able to maintain a constant low temperature to counteract the heating due to friction during MAS.

In this tutorial, a sample of MxiH needles (83 amino acids) was used. This sample was expressed and purified following the protocol established for S. typhimurium PrgI needles.[5] The N-terminal hepta-histidine (His) tag was cleaved using tobacco etch virus protease. The protein concentration was raised to 0.2 mM during polymerization (37°C, 16 days) into needles.

Approximately 20 mg of needle protein were produced with ^{15}NH$_4$Cl as sole nitrogen source and D-[uniform-^{13}C$_6$]-glucose ([U-^{13}C$_6$]Glc) as the sole carbon source. MxiH needles were ultracentrifuged and transferred into a 3.2-mm MAS rotor. Solid-state NMR experiments were conducted on a spectrometer with 700 MHz of ^{1}H Larmor frequency (Bruker Biospin, Germany) at a MAS rate of 17.5 kHz and a sample temperature of 5°C.

4 | PROCEDURE

4.1 | Optimizing the magic angle

Spin up a rotor filled with KBr to 5 kHz. Match and tune the carbon channel to the ^{79}Br transmitter frequency. The peak width at half height of the first sideband should be as low as possible but at least below 130 Hz. The intensity of the first sideband should be roughly 15% of the main signal.

4.2 | Spinning up

Insert the rotor with sample into the spectrometer; make sure that the rotor cap is closed tightly and the rotor cap wings and the mark on the bottom are intact. Half of the rotor bottom edge should be marked black, which is critical for the sensor that measures the MAS frequency.

Increase the MAS frequency stepwise. If the rotor is newly filled, take small steps (e.g., start with 3000 Hz, then steps of 2000 Hz) and monitor the bearing and drive pressure. Leave the sample spinning at each speed for about 3 min for equilibration and prevention of a rotor crash. During the process of spinning up, check the sample temperature after each step to make sure the protein does not overheat or freeze.

Because the sample temperature inside the rotor cannot be measured directly, it is monitored by determining the chemical shift of the H$_2$O signal. For this purpose, 1D proton spectra have to be acquired. Take care to reference your spectra first by setting the DSS peak to a proton

chemical shift of zero. The water peak usually is the strongest signal in the ^1H spectrum and should appear at roughly 5 ppm.

The following equation for temperature calibration (Equation 4)[32,33] also takes the effect of pH and salt concentration (c_{salt}, in mM) into account and is valid in the range 0–80°C, from pH units 2 to 7, and for salt concentrations from 0.0 to 1.0 M.

$$T = \begin{cases} 0°C < T \leq 52°C, & 470.7°C - 93.8\dfrac{°C}{ppm} \cdot \left[\delta_{H_2O} - 0.002\dfrac{ppm}{pH\ unit} \cdot (pH - 7.4) - 9 \times 10^{-5}\dfrac{ppm}{mM} \cdot c_{salt} \right] \\[2ex] 52°C < T \leq 80°C, & 568.8°C - 115.8\dfrac{°C}{ppm} \cdot \left[\delta_{H_2O} - 0.002\dfrac{ppm}{pH\ unit} \cdot (pH - 7.4) - 9 \times 10^{-5}\dfrac{ppm}{mM} \cdot c_{salt} \right] \end{cases} \quad (4)$$

As a rule of thumb, a water peak chemical shift of 4.96 ppm at pH 7 and moderate salt concentrations (around 200 mM) corresponds to a sample temperature of ~5°C. A lower chemical shift corresponds to higher temperatures and vice versa with Δ 0.011 ppm $\approx \Delta$ 1°C. If the sample freezes, the water peak broadens strongly and the signal intensity decreases, whereas in the case of a solvent loss, it will also decrease in intensity but not necessarily broaden. Protein denaturation due to heating leads to broadening of the protein resonances because of increased conformational heterogeneity. Regularly acquired, the ^1H spectrum of DSS will serve as a reference spectrum to monitor and correct the external magnetic field drift.

When the desired MAS speed is reached, make sure that the proton, carbon, and nitrogen channels are matched and tuned correctly.

All experiments in this tutorial were measured on a spectrometer with 700 MHz of ^1H Larmor frequency (Bruker Biospin, Germany) at a MAS rate of 17.5 kHz.
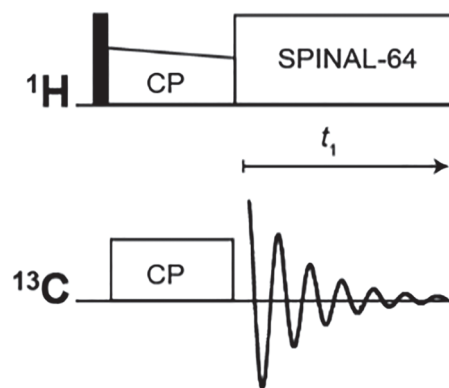
4.3 | Acquisition of a 1D (H)C spectrum ●TIMING 1h

The pulse sequence for this experiment is shown schematically in Figure 4. Data S1 contains the full pulse sequence code. Optimized parameters for this experiment that can act as a guideline are listed in Table 3. The 90° RF field amplitudes used in the following experiments were 83.3, 50, and 35.7 kHz on ^1H, ^{13}C, and ^{15}N, respectively. This equals a 90° pulse duration of 3 μs for ^1H, 5 μs for ^{13}C, and 7 μs for ^{15}N.

1. Set the offset of the proton channel to the water signal (~5 ppm), the offset of the carbon channel to the center of the carbon spectrum (~100 ppm), and the offset of the nitrogen channel to the center of the backbone nitrogen signal (~120 ppm).
2. Set an initial 90° proton excitation pulse length to 3 μs (83.3 kHz) and set the corresponding power level.
3. Calculate and set a possible condition for CP that fulfills the Hartmann–Hahn condition ($|\omega_{NucA} \pm \omega_{NucB}| = n \cdot \omega_{MAS}$, with ω being the radio frequency field strength of the nucleus A or B, ω_{MAS} being the


FIGURE 4 Schematic representation of the (H)C correlation experiment pulse sequence. Filled rectangles represent 90° pulses

TABLE 3 Set of optimized experimental parameters for the acquisition of a 1D (H)C spectrum

Parameter	Value
Initial transfer	HC-CP
Field (kHz)-H	74.6
Field (kHz)-C	50
Pulse shape	Ramp 100–80% on H
Time (ms)	0.2/0.6/1
Detection (t_1)	C
Field (kHz)-H	82.8

MAS frequency, and $n = 1$ or $n = 2$). Avoid resonance and/or recoupling conditions for any of the involved nuclei ($\omega_{Nuc}/\omega_{MAS} = 0.5, 1,$ or 2). A useful starting point for the carbon CP pulse is the carbon 90° pulse RF (50 kHz). If a ramp-shaped pulse is used, set the pulse power level so that the theoretical optimum is reached in the middle of the ramp.

4. Use SPINAL-64[34] decoupling on the proton channel during acquisition.
5. Set the duration of the SPINAL-64 165° decoupling pulses to 5.6 μs and the corresponding power level.
6. Set the acquisition time to 15 ms.
7. Set the spectral width to span the whole carbon spectrum (~300 ppm).
8. Set the number of scans to an integer multiple of the number of phase cycle steps. Set the recycle delay to 2 s.
9. Optimize the first proton 90° excitation pulse (see Box 1).
10. Optimize the carbon 90° pulse (see Box 1).
11. Optimize the power levels and contact time of the CP step, the slope, the channel, and the direction of the CP ramp and the SPINAL-64 decoupling pulse length and power level (starting from the optimized proton 90° pulse power level and looking for maximum resolution). In addition, optimize the CP contact time once for optimal CA and once for optimal CO signal. These spectra can serve as reference spectra to determine transfer efficiencies.
12. Acquire the 1D (H)C spectrum (Figure 5) using the optimized values. Regularly acquired (e.g., between multidimensional experiments) it will serve as a reference spectrum to monitor sample and spectrometer stability.
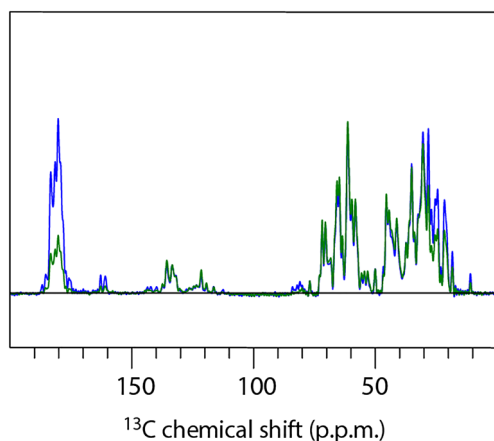
FIGURE 5 (H)C spectrum of uniformly $^{13}C-^{15}N$-labeled MxiH needles (83aa) in a 3.2-mm rotor at 17.5-kHz MAS using 32 scans with a CP contact time of 200 μs (green) for high CA and 1000 μs (blue) for high CO signal as reference spectra

---

Box 1. How to optimize the 90° pulses

^{1}H: Double the duration of the proton pulse (90–80° H pulse), and try to get the signal as close to zero as possible by varying either the power level or the duration.

Do not forget to set the duration of the proton pulse back to half the optimized value for a 90° pulse when finished.

^{13}C and ^{15}N: For optimizing the carbon 90° pulse, set the RF offset to the center of the CO signal and include a carbon 90° pulse after the (H)C step. For optimizing the nitrogen 90° pulse, just add a nitrogen 90° pulse to the (H)N experiment.

Try to eliminate the signal by varying either the power level or the duration of the pulse.

Do not forget to delete the 90° pulse again when finished, and set the carbon offset back to the center of the whole carbon region.

4.4 | Acquisition of a 2D (H)CC correlation PDSD spectrum ●TIMING 1d

The pulse sequence for this experiment is shown schematically in Figure 6. Data S2 contains the full pulse sequence code. Optimized parameters for this experiment that can act as a guideline are listed in Table 4.

13. Use the offset parameters from Step 1 for the setup of this experiment.
14. Use the optimized parameters (pulse lengths, power levels, etc.) from the (H)C 1D experiment. The easiest way to keep the optimized values from the (H)C is to copy the (H)C experiment into a new experiment number, change it into a 2D experiment, and then read in the (H)CC PDSD pulse sequence.
15. Set the duration of the carbon 90° pulses to 5 μs and set the corresponding power level.
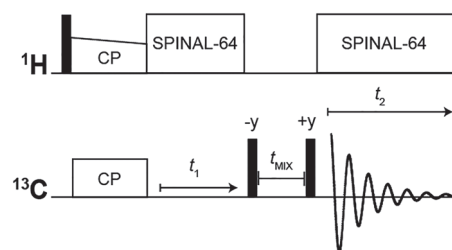
FIGURE 6 Schematic representation of the (H)CC PDSD experiment pulse sequence. Filled rectangles represent 90° pulses

TABLE 4 Set of optimized experimental parameters for the acquisition of a 2D (H)CC spectrum

Parameter	Value
Second transfer	C-C PDSD
Field (kHz)-C	50
^{13}C carrier (ppm)	65
Mixing time (ms)	50
t_1 evolution	C
Field (kHz)-H	82.2
Spectral width	46 kHz/261 ppm
Acquisition time (ms)	10
Detection (t_2)	C
Field (kHz)-H	82.8

16. Set the mixing time for the PDSD to 50 ms.
17. Set the acquisition times. Useful values could be ~12 ms for the direct dimension and ~10 ms for the indirect dimension. To optimize the acquisition times, inspect the signal decay in the free induction decay.
18. Set the spectral widths in the direct and indirect dimensions to cover the whole carbon spectrum.

Optional: Set a frequency constant so that the carrier frequency is shifted to the center of the CA region during acquisition of the indirect dimension and reduce the spectral width to the CA and side-chain C region. Note: Reducing the spectral width in the indirect dimension saves measurement time, but the CO signals will be folded into the spectrum. Adjusting the spectral width carefully prevents overlap of the folded CO signals with other important resonances.

19. Set the number of scans to 32 and the number of dummy scans to 16. Set the recycle delay to 2 s.
20. Acquire the 2D (H)CC PDSD NMR spectrum (Figure 7) using the optimized values. This spectrum can serve as a fingerprint spectrum to compare the sample to previous samples of the same protein. Acquired with higher mixing times (up to 200 ms) and ideally at lower spinning speed (11 kHz), PDSD spectra can provide not only intraresidue but also long-distance cross peaks.

## 4.5 | Acquisition of a 1D (H)N spectrum ●TIMING 1h

The pulse sequence for this experiment is shown schematically in Figure 8a. Data S3 contains the full pulse
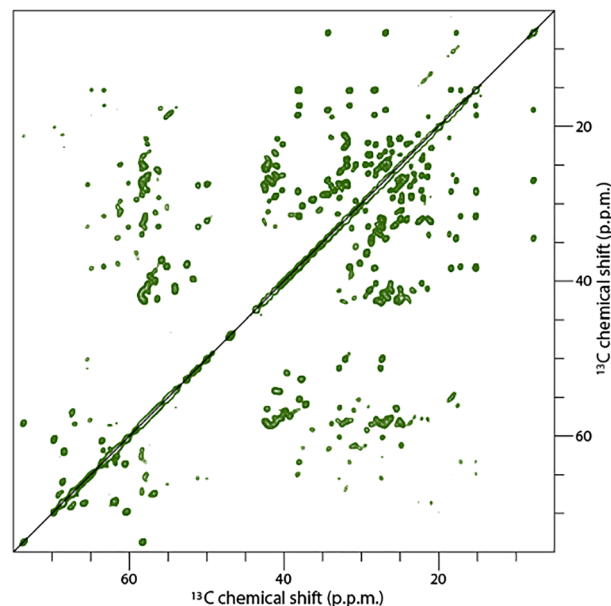
FIGURE 7 (H)CC PDSD spectrum of uniformly ^{13}C–^{15}N-labeled MxiH needles (83aa) in a 3.2-mm rotor at 17.5-kHz MAS with 32 scans per t_1 experiment. This spectrum helps to assess the overall quality that is achievable for the spectra recorded of one specific sample

sequence code. Optimized parameters for this experiment that can act as a guideline are listed in Table 5.

21. Use the offset parameters from Step 1 for the setup of this experiment.
22. Set the first 90° proton excitation pulse and the SPINAL-64 decoupling pulse length and power level to the optimized values from the (H)C 1D experiment.
23. Calculate and set a possible condition for CP that fulfills the Hartmann–Hahn condition ($|\omega_{NucA} \pm \omega_{NucB}| = n \cdot \omega_{MAS}$, with ω being the radio frequency field strength of the nucleus A or B, ω_{MAS} being the MAS frequency, and $n = 1$ or $n = 2$). Avoid resonance and/or recoupling conditions for any of the involved nuclei ($\omega_{Nuc}/\omega_{MAS} = 0.5$, 1, or 2). A useful starting point for the nitrogen CP pulse is the nitrogen 90° pulse RF (35.7 kHz).
24. Set the spectral width to span the whole nitrogen spectrum (~40 ppm for the backbone at 120 ppm, additional side-chain signals are expected as well, e.g., from Lys at 30 ppm). Set the acquisition time to 15 ms.
25. Set the number of scans to an integer multiple of the number of phase cycle steps. Set the recycle delay to 2 s.
26. Optimize the nitrogen 90° pulse (see Box 1).

(a)

(b)
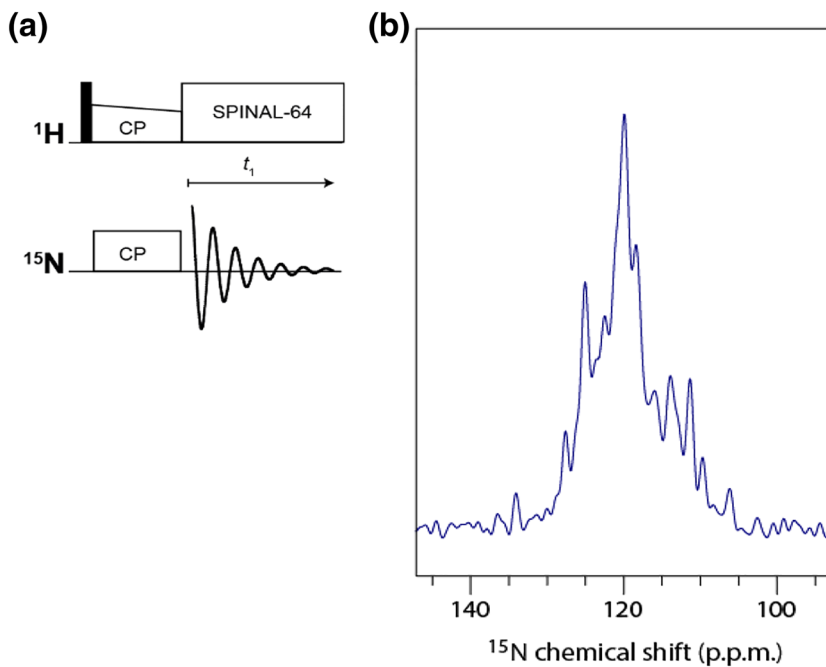
FIGURE 8 (a) Schematic representation of the (H)N correlation experiment pulse sequence. Filled rectangles represent 90° pulses. (b) (H)N spectrum of uniformly ^{13}C–^{15}N-labeled MxiH needles (83aa) in a 3.2-mm rotor at 17.5-kHz MAS using 32 scans

**TABLE 5** Set of optimized experimental parameters for the acquisition of a 1D (H)N spectrum

Parameter	Value
Initial transfer	HN-CP
Field (kHz)-H	59.3
Field (kHz)-N	38.7
Pulse shape	Ramp 100–80% on H
Time (ms)	0.65
Detection (t_1)	N
Field (kHz)-H	82.8

27. Optimize the power levels and contact time of the CP step, the slope, the channel, and the direction of the CP ramp.
28. Acquire the 1D (H)N spectrum (Figure 8b) using the optimized values.

4.6 | Acquisition of 1D and 2D (H)NCA spectra ●TIMING 6h

The pulse sequence for this experiment is shown schematically in Figure 9. Data S4 contains the full pulse sequence code. Optimized parameters for this experiment that can act as a guideline are listed in Table 6.

29. Use the offset parameters from Step 1 for the setup of this experiment.
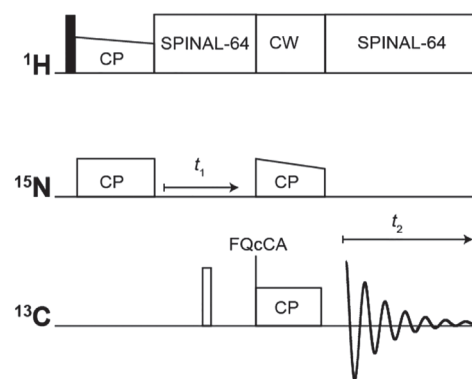
FIGURE 9 Schematic representation of the (H)NCA correlation experiment pulse sequence. Filled rectangles represent 90° pulses and empty rectangles 180° pulses

30. Set the first 90° proton excitation pulse to the optimized values from the (H)N 1D experiment.
31. Set a constant that shifts the carbon carrier frequency to the center of the CA region before the NC-CP step.
32. Calculate and set a possible condition for the SPECIFIC-CP that fulfills the Hartmann–Hahn condition ($|\omega_{NucA} + \omega_{NucB}| = \omega_{MAS}$, with ω being the radio frequency field strength of the nucleus A or B and ω_{MAS} being the MAS frequency) for nitrogen to CA. Avoid resonance and/or recoupling conditions for any of the involved nuclei ($\omega_{Nuc}/\omega_{MAS} = 0.5$ or 1). Use low power pulses to avoid unspecific transfer. A useful contact time can be 3 ms.

TABLE 6   Set of optimized experimental parameters for the acquisition of a 2D (H)NCA spectrum

Parameter	Value
Second transfer	NCA SPECIFIC-CP
Field (kHz)-H	85.0
Field (kHz)-N	5.6
Field (kHz)-C	13.0
Pulse shape	Ramp 80–100% on C
^{13}C carrier (ppm)	65
Time (ms)	4.6
t_1 evolution	N
Field (kHz)-H	82.8
180° pulse	C
Spectral width	7 kHz/99 ppm
Acquisition time (ms)	12
Detection (t_2)	CA
Field (kHz)-H	82.8

33. Use continuous wave (CW)[35] decoupling on the proton channel during the NCA SPECIFIC-CP transfer. Use SPINAL-64 decoupling during acquisition. The SPINAL-64 decoupling pulses can be set to the optimized parameters from Step 11.
34. Set the acquisition times to 10 ms in the direct and 15 ms in the indirect dimension.
35. Set the spectral widths to span the whole carbon spectrum (~300 ppm) in the direct dimension and to span the whole nitrogen region (~40 ppm) in the indirect dimension.
36. Set the number of scans to 32. Set the recycle delay to 2 s.
37. Use the 1D (H)NCA experiment to optimize the power levels and the duration of the NC-CP step, the slope, the channel, and the direction of the CP ramp, and the CW decoupling pulse power level.
38. Acquire a 1D (H)NCA spectrum using the optimized values. This spectrum can serve as a reference spectrum to determine transfer efficiency. For this purpose, compare the intensity of the spectrum in the CA region to the 1D (H)C spectrum with optimal CA signal. A transfer efficiency of ~30% is considered good.
39. Set the number of scans to 128 and the number of dummy scans to 16. Set the recycle delay to 2 s.
40. Acquire a 2D (H)NCA spectrum (Figure 10). This spectrum can be used to further optimize the spectral widths to save acquisition times in 3D experiments.
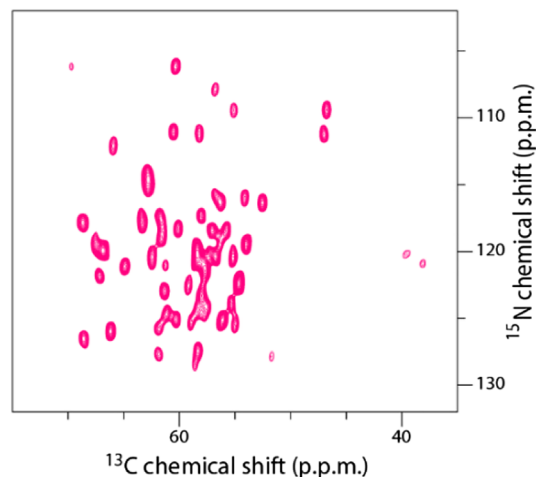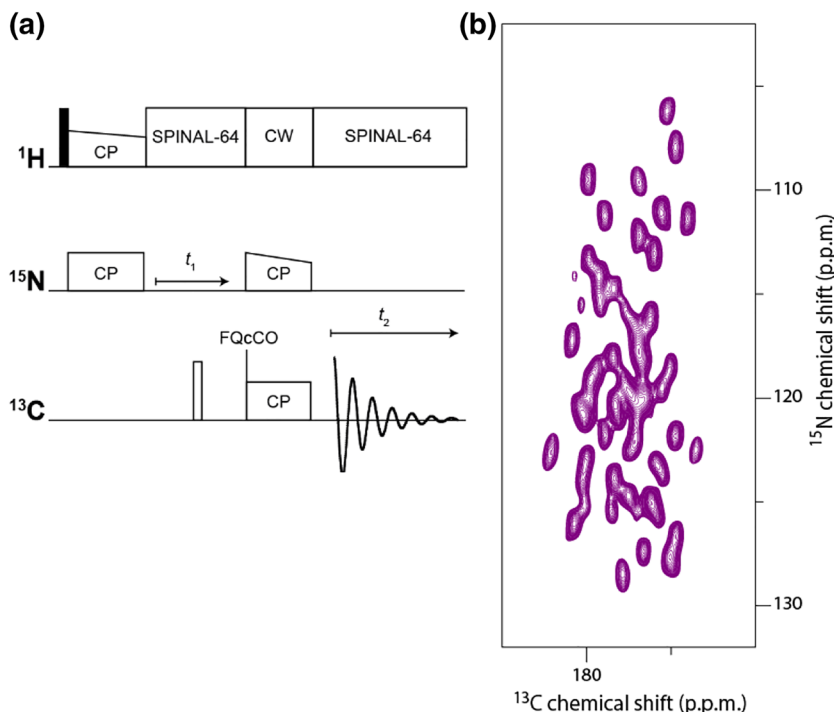

FIGURE 10   2D (H)NCA spectrum of uniformly ^{13}C–^{15}N-labeled MxiH needles (83aa) in a 3.2-mm rotor at 17.5-kHz MAS

4.7 | Acquisition of 1D and 2D (H)NCO spectra ●TIMING 6h

The pulse sequence for this experiment is shown schematically in Figure 11a. Data S4 contains the full pulse sequence code. Optimized parameters for this experiment that can act as a guideline are listed in Table 7.

41. Use the offset parameters from Step 1 for the setup of this experiment.
42. Use all the optimized power levels and contact times from the (H)NCA experiment.
43. Set a constant that shifts the carbon carrier frequency to the center of the CO region before the NC-CP step.
44. Use CW decoupling on the proton channel during the CP transfer. Use SPINAL-64 decoupling during acquisition.
45. Set the acquisition times to 10 ms in the direct and 15 ms in the indirect dimension.
46. Set the spectral widths to span the whole carbon spectrum (~300 ppm) in the direct dimension and to span the whole nitrogen region (~40 ppm) in the indirect dimension.
47. Set the number of scans to 32. Set the recycle delay to 2 s.
48. Use the 1D (H)NCO experiment to optimize the power levels and the duration of the NCO SPECIFIC-CP step, the slope, the channel, and the direction of the CP ramp.

Attention: The parameters of the NCO transfer can be significantly different from the NCA transfer!

(a)   **(b)**

FIGURE 11 (a) Schematic representation of the (H)NCO correlation experiment pulse sequence. Filled rectangles represent 90° pulses and empty rectangles 180° pulses. (b) 2D (H)NCO spectrum of uniformly ^{13}C–^{15}N-labeled MxiH needles (83aa) in a 3.2-mm rotor at 17.5-kHz MAS

TABLE 7 Set of optimized experimental parameters for the acquisition of a 2D (H)NCO spectrum

| Parameter	Value
Second transfer	NCO SPECIFIC-CP
Field (kHz)-H	88.7
Field (kHz)-N	7.9
Field (kHz)-C	10.3
Pulse shape	Ramp 100–80% on N
^{13}C carrier (ppm)	185.2
Time (ms)	3.8
t_1 evolution	N
Field (kHz)-H	82.8
180° pulse	C
Spectral width	7 kHz/99 ppm
Acquisition time (ms)	12
Detection (t_2)	CO
Field (kHz)-H	82.2

49. Acquire a 1D (H)NCO spectrum using the optimized values. This spectrum can serve as a reference spectrum to determine transfer efficiency. For this purpose, compare the intensity of the spectrum in the CO region to the 1D (H)C spectrum with optimal CO signal. A transfer efficiency of ~30% is considered good.

50. Set the number of scans to 128 and the number of dummy scans to 16. Set the recycle delay to 2 s.

51. Acquire a 2D (H)NCO spectrum (Figure 11b). This spectrum can be used to further optimize the spectral widths to save acquisition times in 3D experiments.

4.8 | Acquisition of a 3D (H)NCACO spectrum ●TIMING 2d

The pulse sequence for this experiment is shown schematically in Figure 12a. Data S5 contains the full pulse sequence code. Optimized parameters for this experiment that can act as a guideline are listed in Table 8.

52. Use the offset parameters from Step 1 for the setup of this experiment.

53. Use all the optimized parameters from the 2D (H)NCA experiment.

54. Calculate and set the pulses for the BSH-CP transfer (see Box 2). The BSH-CP contact time should be ~3 ms.

55. Set two constants, one that shifts the carbon carrier frequency to the center of the CA region before the NC-CP step and one after the BSH-CP transfer that shifts the carbon carrier frequency to the center of the CO region before the trim pulse.

(a)

(b)
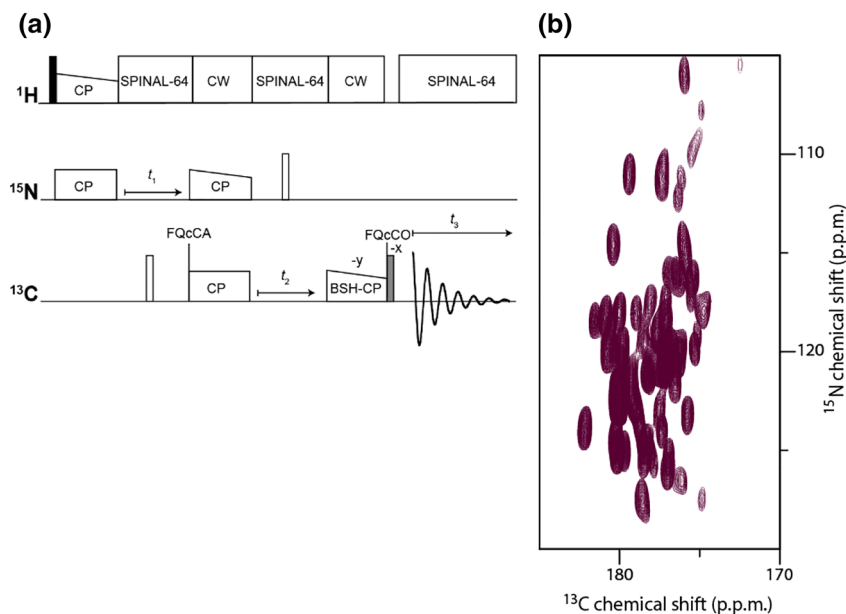
FIGURE 12 (a) Schematic representation of the 3D (H)NCACO correlation experiment pulse sequence. Filled, empty, and gray rectangles represent 90° pulses, 180° pulses, and trim pulses, respectively. (b) 2D projection of the 3D (H)NCACO spectrum of uniformly ^{13}C–^{15}N-labeled MxiH needles (83aa) in a 3.2-mm rotor at 17.5-kHz MAS, projection along the ^{13}CO–^{15}N plane over the whole ^{13}CA chemical shift range

TABLE 8 Set of optimized experimental parameters for the acquisition of a 3D (H)NCACO spectrum

Parameter	Value
t_1 evolution	N
Field (kHz)-H	83.3
180° pulse	C
Spectral width	3.6 kHz/50 ppm
Acquisition time (ms)	6
Third transfer	CA–CO BSH-CP
Field (kHz)-H	83.3
Field (kHz)-C	10.9
Pulse shape	Ramp 100–80% on C
^{13}C carrier (ppm)	60.8
Time (ms)	3.8
Trim pulse	3.4 µs/50 kHz
t_2 evolution	CA
Field (kHz)-H	83.3
180° pulse	N
Spectral width	6 kHz/34 ppm
Acquisition time (ms)	5
Detection (t_3)	C
Field (kHz)-H	83.3

56. Set the acquisition times to 10 ms for the direct dimension, 5 ms for the carbon indirect dimension, and 6 ms for the nitrogen indirect dimension. If measurement time is limited, shortening the acquisition times in the indirect dimensions can be useful to shorten the experiment time.

Set the spectral widths to span the whole carbon spectrum in the direct dimension, the whole CA region in the carbon indirect dimension and the whole amide nitrogen range in the nitrogen indirect dimension. The spectral widths for the indirect dimensions can be extracted from the 2D (H)NCA. To save measurement time, limit the indirect spectral widths as much as possible.

57. Use CW decoupling on the proton channel during the CP transfer. Use SPINAL-64 decoupling during acquisition.
58. Set the number of scans to an integer multiple of the number of phase cycle steps. Set the recycle delay to 2 s.
59. To optimize the power level and the duration of the BSH-CP transfer step, the slope, and the direction of the CP ramp and the decoupling power level, acquire the 1D version of the (H)NCACO spectrum and optimize for maximal negative CO signal. This spectrum can serve as a reference spectrum to determine transfer efficiency if recorded with the same number of scans as the other 1D reference spectra (32 scans). To determine the transfer efficiency of the BSH-CP step, compare the intensity of the spectrum in the CO region to the 1D (H)NCO spectrum. A transfer efficiency of ~30% is considered good, up to 40% can be achieved.
60. Optimize the necessary acquisition times in the indirect dimensions by acquiring the 2D (H)

NCACO versions of the spectrum. Set the size of the free induction decay to one for either nitrogen or CA.

61. Set the number of dummy scans to 16 and acquire a 3D (H)NCACO spectrum (Figures 12b and 13) using the optimized values.

Box 2 How to calculate the conditions for the BSH-CP transfer

The theoretical RF field amplitude ω_{rf} of the BSH-CP pulse is given by

$$\omega_{eff} + \omega_{rf} = 2\omega_r$$

with ω_{eff} being the effective field on CO and ω_r being the MAS spinning frequency. Because

$$\omega_{eff} = \sqrt{\Omega^2 + \omega_{rf}^2}$$

with Ω being the difference of the CA and CO chemical shift offsets in Hz, ω_{rf} can be calculated as

$$\sqrt{\Omega^2 + \omega_{rf}^2} + \omega_{rf} = 2\omega_r$$

so that

$$\omega_{rf} = \frac{4\omega_r^2 - \Omega^2}{4\omega_r} = \omega_r - \frac{\Omega^2}{4\omega_r}$$

For magnetization transfer from CA to CO, a hard trim pulse on CO has to be applied after the BSH-CP step to selectively flip the CO magnetization to the transverse plane for acquisition.

The power level of the trim pulse can be set to the power level of the optimized carbon 90° pulse, and the duration of the trim pulse p_{tp} can easily be calculated from the carbon 90° pulse duration p_{90}:

$$p_{tp} = p_{90} \cdot \frac{\theta}{90°}$$

via the flip angle θ which is given by

$$\theta = \arctan\left(\frac{\Omega}{\omega_{rf}}\right)$$

For BSH-CP transfer from CO to CA, the trim pulse is necessary before BSH-CP to flip the CO magnetization along the effective field.
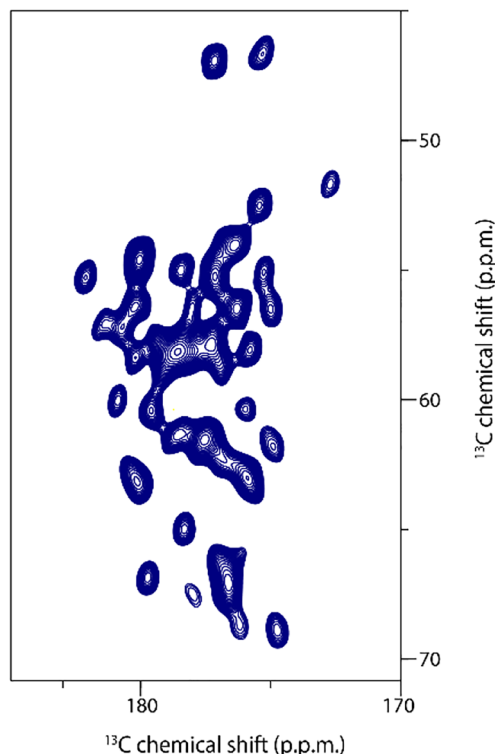

FIGURE 13 2D projection of the 3D (H)NCACO spectrum of uniformly ^{13}C–^{15}N-labeled MxiH needles (83aa) in a 3.2-mm rotor at 17.5-kHz MAS, projection along the ^{13}CO–^{13}CA plane over the whole ^{15}N chemical shift range

4.9 | Acquisition of a 3D (H)NCACB spectrum ●TIMING 2d

The pulse sequence for this experiment is shown schematically in Figure 14. Data S6 contains the full pulse sequence code. Optimized parameters for this experiment that can act as a guideline are listed in Table 9.

62. Use the offset parameters from Step 1 for the setup of this experiment.
63. Use all the optimized parameters (power levels, contact times, and frequency constants) from the (H) NCA experiment.
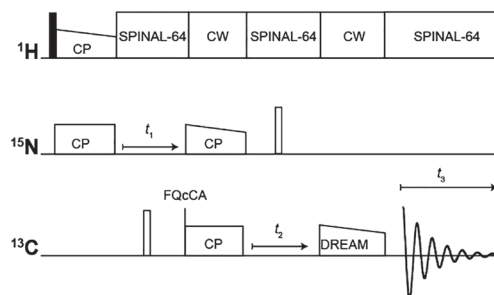

FIGURE 14 Schematic representation of the 3D (H)NCACB correlation experiment pulse sequence. Filled and empty rectangles represent 90° and 180° pulses, respectively

TABLE 9 Set of optimized experimental parameters for the acquisition of a 3D (H)NCACB spectrum

Parameter	Value
t_1 evolution	N
Field (kHz)-H	82.8
180° pulse	C
Spectral width	2 kHz/28 ppm
Acquisition time (ms)	6
Third transfer	CA–CB DREAM
Field (kHz)-H	86.7
Field (kHz)-C	8.8
Pulse shape	Ramp 100–80% on C
^{13}C carrier (ppm)	65
Time (ms)	1.8
t_2 evolution	CA
Field (kHz)-H	82.8
180° pulse	N
Spectral width	4 kHz/23 ppm
Acquisition time (ms)	5
Detection (t_3)	CA, CB
Field (kHz)-H	82.2

64. Set the pulse for the DREAM transfer. The RF field on carbon should be half of the spinning speed for the transfer.
65. Set the acquisition times to 10 ms for the direct dimension, 5 ms for the carbon indirect dimension, and 6 ms for the nitrogen indirect dimension.
66. Set the spectral widths to span the whole carbon spectrum in the direct dimension, the whole CA region in the carbon indirect dimension, and the whole amide nitrogen range in the nitrogen indirect dimension. The spectral widths for the indirect dimensions can be extracted from the 2D (H)NCA. To save measurement time, reduce the spectral widths as much as possible (considering folding peaks).
67. Use CW decoupling on the proton channel during the NCA SPECIFIC-CP and the DREAM transfer. Use SPINAL-64 decoupling during chemical shift evolution periods.
68. Set the number of scans to an integer multiple of the phase cycle step number. Set the recycle delay to 2 s.
69. To maximize the DREAM transfer efficiency, acquire the 1D version of the (H)NCACB spectrum and optimize for maximum negative CB signal by varying the DREAM pulse ramp, the power level, the duration, and the decoupling power level. This
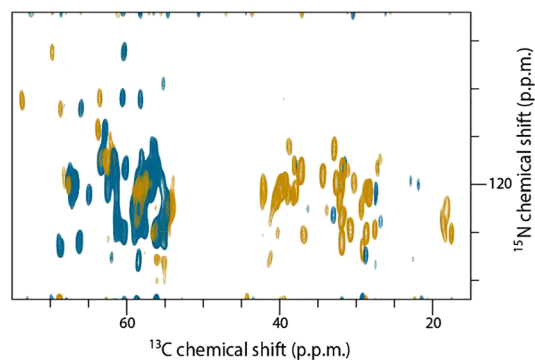
FIGURE 15 3D (H)NCACB spectrum of uniformly ^{13}C–^{15}N-labeled MxiH needles (83aa) in a 3.2-mm rotor at 17.5-kHz MAS, 2D projection along the ^{13}CB–^{15}N plane over the whole ^{13}CA chemical shift range. Positive signals in turquoise represent remaining magnetization on CA nuclei, whereas negative signals in ochre show CB resonances

spectrum can serve as a reference to determine transfer efficiency if recorded with the same number of scans as the 1D reference spectra (32 scans).
70. Optimize the necessary acquisition times in the indirect dimensions by acquiring the 2D (H)NCACB versions of the spectrum.
71. Set the number of dummy scans to 16 and acquire a 3D (H)NCACB spectrum (Figure 15) using the optimized values.

4.10 | Acquisition of a 3D (H)CANCO spectrum ●TIMING 2d

The pulse sequence for this experiment is shown schematically in Figure 16. Data S7 contains the full pulse sequence code. Optimized parameters for this experiment that can act as a guideline are listed in Table 10.

72. Use the offset parameters from Step 1 for the setup of this experiment.
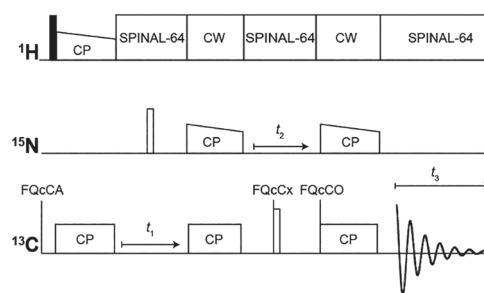
FIGURE 16 Schematic representation of the 3D (H)CANCO correlation experiment pulse sequence. Filled and empty rectangles represent 90° and 180° pulses, respectively

TABLE 10 Set of optimized experimental parameters for the acquisition of a 3D (H)CANCO spectrum

| Parameter	Value
Initial transfer	HCA-CP
Field (kHz)-H	74.7
Field (kHz)-C	50
Pulse shape	Ramp 100–80% on H
^{13}C carrier (ppm)	65.0
Time (ms)	0.175
Second transfer	CAN SPECFIC-CP
Field (kHz)-H	84.7
Field (kHz)-N	7.9
Field (kHz)-C	13.3
Pulse shape	Ramp 100–80 on N
^{13}C carrier (ppm)	65.0
Time (ms)	4.3

73. Use all the optimized parameters from the (H)NCO experiment.

74. Set three frequency constants: one before the first proton 90° pulse that shifts the carrier frequency to the center of the CA region (Figure 16: FQcCA), one that shifts the carrier frequency back to the center of the spectral width (FQcCx), and a constant that shifts the carrier frequency to the center of the CO region after t_2, before the NCO-CP step (FQcCO).

75. Optimize the HCA-CP in a 1D (H)C experiment (power levels, ramp, and pulse length) in which the carrier frequency is set to the center of the CA region and use the optimized parameters for the 3D (H)CANCO experiment.

76. Set the spectral widths to span the whole carbon spectrum in the direct dimension, the whole CA region in the carbon indirect dimension, and the whole amide nitrogen range in the nitrogen indirect dimension. The spectral widths for the indirect dimensions can be extracted from the 2D (H)NCA. To save measurement time, limit the spectral widths as much as possible (considering folding peaks).

77. Use CW decoupling on the proton channel during the CP transfer. Use SPINAL-64 decoupling during acquisition.

78. Set the acquisition times to 10 ms for the direct dimension, 5 ms for the carbon indirect dimension, and 6 ms for the nitrogen indirect dimension.

79. Set the number of scans to an integer multiple of the number of phase cycle steps. Set the recycle delay to 2 s.
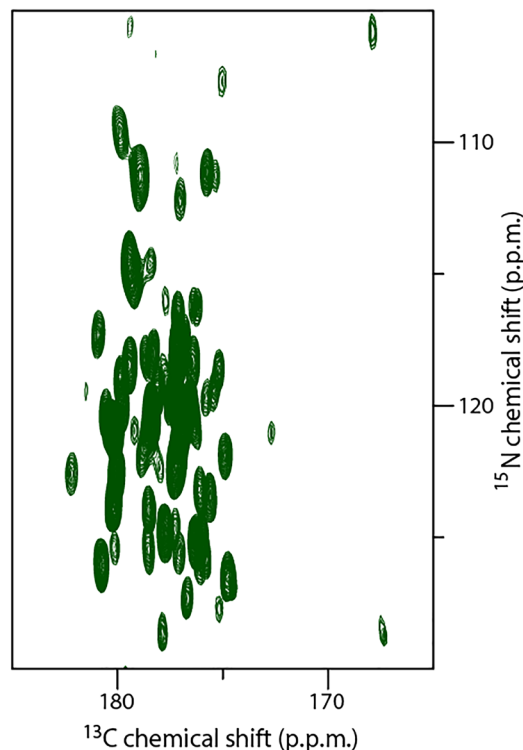
FIGURE 17 3D (H)CANCO spectrum of uniformly ^{13}C–^{15}N-labeled MxiH needles (83aa) in a 3.2-mm rotor at 17.5-kHz MAS, projection along the ^{13}CO–^{15}N plane over the whole ^{13}CA chemical shift range

80. To optimize the power levels and the duration of the CP transfer step from CA to nitrogen, the slope, the channel, and the direction of the CP ramp and the decoupling power level, acquire the 1D version of the (H)CANCO spectrum and optimize for maximal signal. This spectrum can serve as a reference spectrum to determine transfer efficiency if recorded with the same number of scans as the other 1D reference spectra (32 scans). To estimate the transfer efficiency of the CAN SPECIFIC-CP step, compare the intensity of the spectrum in the CO region to the 1D (H)NCO spectrum. Efficiencies of 30% or more are considered good.

81. Optimize the necessary acquisition times in the indirect dimensions by acquiring the 2D (H)CANCO versions of the spectrum.

82. Set the number of dummy scans to 16 and acquire a 3D (H)CANCO spectrum (Figure 17) using the optimized values.

4.11 | Acquisition of a 3D (H)NCOCA spectrum ●TIMING 1d

The pulse sequence for this experiment is shown schematically in Figure 18. Data S8 contains the full pulse
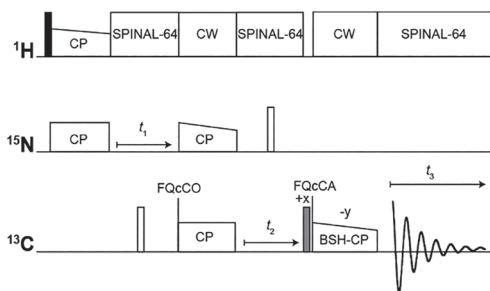
FIGURE 18 Schematic representation of the 3D (H)NCOCA correlation experiment pulse sequence. Filled, empty, and gray rectangles represent 90° pulses, 180° pulses, and trim pulses, respectively

sequence code. Optimized parameters for this experiment that can act as a guideline are listed in Table 11.

83. Use the offset parameters from Step 1 for the setup of this experiment.
84. Use all the optimized parameters (power levels and contact times) from the (H)NCO experiment.
85. Set the pulses for the BSH-CP transfer (see Box 2). The power levels and the pulse lengths can be adopted from the (H)NCACO experiment.

TABLE 11 Set of optimized experimental parameters for the acquisition of a 3D (H)NCOCA spectrum

Parameter	Value
t_1 evolution	N
Field (kHz)-H	82.8
180° pulse	C
Spectral width	2 kHz/28 ppm
Acquisition time (ms)	6
Third transfer	CO–CA BSH-CP
Trim pulse	3.25 μs/50 kHz
Field (kHz)-H	85.7
Field (kHz)-C	11.7
Pulse shape	Ramp 100–80 on C
^{13}C carrier (ppm)	65
Time (ms)	3.7
t_2 evolution	CO
Field (kHz)-H	82.8
180° pulse	N
Spectral width	2 kHz/11 ppm
Acquisition time (ms)	5
Detection (t_3)	C
Field (kHz)-H	82.2

86. Set a constant that shifts the carbon carrier frequency to the center of the CO region before the NC-CP step and a constant that shifts the carbon carrier frequency to the center of the CA region before the BSH-CP step.
87. Use CW decoupling on the proton channel during the CP and BSH-CP transfers. Use SPINAL-64 decoupling during the chemical shift evolution periods.
88. Set the acquisition times to 10 ms for the direct dimension, 5 ms for the carbon indirect dimension, and 6 ms for the nitrogen indirect dimension.
89. Set the spectral widths to span the whole carbon spectrum in the direct dimension, the whole CO region in the carbon indirect dimension, and the whole amide nitrogen range in the nitrogen indirect dimension. The spectral widths for the indirect dimensions can be extracted from the 2D (H)NCO. To save measurement time, limit the spectral widths as much as possible (considering folding-in of peaks).
90. Set the number of scans to an integer multiple of the phase cycle step number. Set the recycle delay to 2 s.
91. To optimize the power level and the duration of the BSH-CP transfer step, the slope, and the direction of the BSH-CP ramp and the decoupling power level, acquire the 1D version of the (H) NCOCA spectrum and optimize for maximal signal. This spectrum can serve as a reference spectrum to determine transfer efficiency if recorded with the same number of scans as the other 1D reference spectra (32 scans). To estimate the transfer efficiency of the CO–CA BSH-CP step, compare the intensity of the spectrum in the CA region to the 1D (H)NCA spectrum. Efficiencies of 30% or more are considered good.
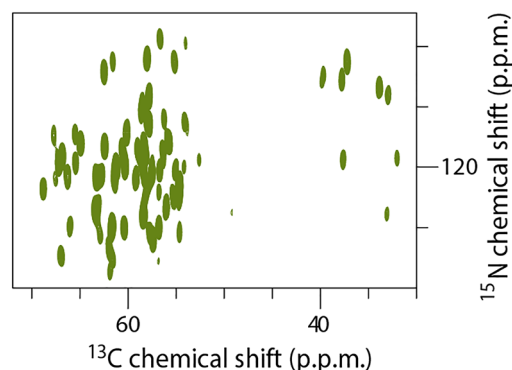

FIGURE 19 3D (H)NCOCA spectrum of uniformly ^{13}C–^{15}N-labeled MxiH needles (83aa) in a 3.2-mm rotor at 17.5-kHz MAS, 2D projection along the ^{13}CA–^{15}N plane over the whole ^{13}CO chemical shift range

92. Optimize the necessary acquisition times in the indirect dimensions by acquiring the 2D (H)NCOCA versions of the spectrum.
93. Acquire a 3D (H)NCOCA spectrum (Figure 19) using the optimized values.

4.12 | Acquisition of a 3D (H)NCO(CA)CB spectrum ●TIMING 1d

The pulse sequence for this experiment is shown schematically in Figure 20. Data S9 contains the full pulse sequence code. Optimized parameters for this experiment that can act as a guideline are listed in Table 12.

94. Use the offset parameters from Step 1 for the setup of this experiment.
95. Use all the optimized power levels and contact times from the (H)NCOCA experiment.
96. Adopt the optimized values for the power levels and the duration of the DREAM transfer step from the (H)NCACB experiment.
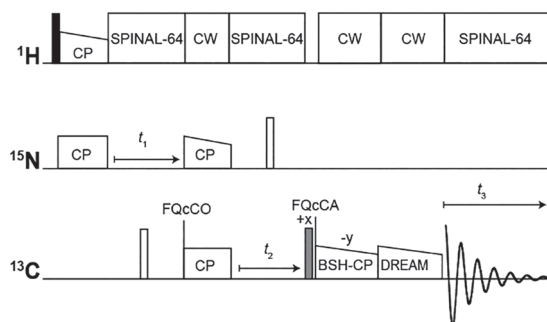
FIGURE 20 Schematic representation of the 3D (H)NCO(CA)CB correlation experiment pulse sequence. Filled, empty, and gray rectangles represent 90°, 180°, and trim pulses, respectively

TABLE 12 Set of optimized experimental parameters for the acquisition of a 3D (H)NCO(CA)CB spectrum

| Parameter	Value
Fourth transfer	CA–CB DREAM
Field (kHz)-H	86.7
Field (kHz)-C	8.8
Pulse shape	Ramp 100–80% on C
^{13}C carrier (ppm)	65
Time (ms)	1.8
Detection (t_3)	C
Field (kHz)-H	82.2
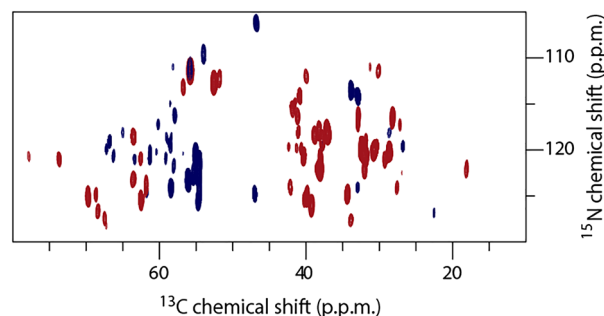
FIGURE 21 3D (H)NCO(CA)CB spectrum of uniformly ^{13}C–^{15}N-labeled MxiH needles (83aa) in a 3.2-mm rotor at 17.5-kHz MAS, projection along the ^{13}CB–^{15}N plane over the whole ^{13}CO chemical shift range. Positive signals in dark blue represent remaining magnetization on CA nuclei, whereas negative signals in dark red show CB resonances

97. Use CW decoupling on the proton channel during the CP transfer. Use SPINAL-64 decoupling during acquisition.
98. Set the acquisition times to 10 ms for the direct dimension, 5 ms for the carbon indirect dimension, and 6 ms for the nitrogen indirect dimension.
99. Set the spectral widths to span the whole carbon spectrum in the direct dimension, the whole CO region in the carbon indirect dimension, and the whole amide nitrogen range in the nitrogen indirect dimension. The spectral widths for the indirect dimensions can be extracted from the 2D (H)NCO. To save measurement time, narrow the spectral widths as much as possible (considering folding-in of peaks).
100. Set the number of scans to an integer multiple of the number of phase cycle steps. Set the recycle delay to 2 s.
101. Acquire the 1D version of the (H)NCO(CA)CB. This spectrum can also serve as reference spectrum to determine the transfer efficiency if recorded with the same number of scans as the other 1D reference spectra (32 scans).
102. Optimize the necessary acquisition times in the indirect dimensions by acquiring the 2D (H)NCO(CA)CB versions of the spectrum.
103. Set the number of dummy scans to 16. Using the optimized parameters, acquire the 3D (H)NCO(CA)CB spectrum (Figure 21).

4.13 | Acquisition of a 3D (H)N(CO)CACB spectrum ●TIMING 2d

The pulse sequence for this experiment is shown schematically in Figure 22a. Data S10 contains the full pulse

(a)

(b)
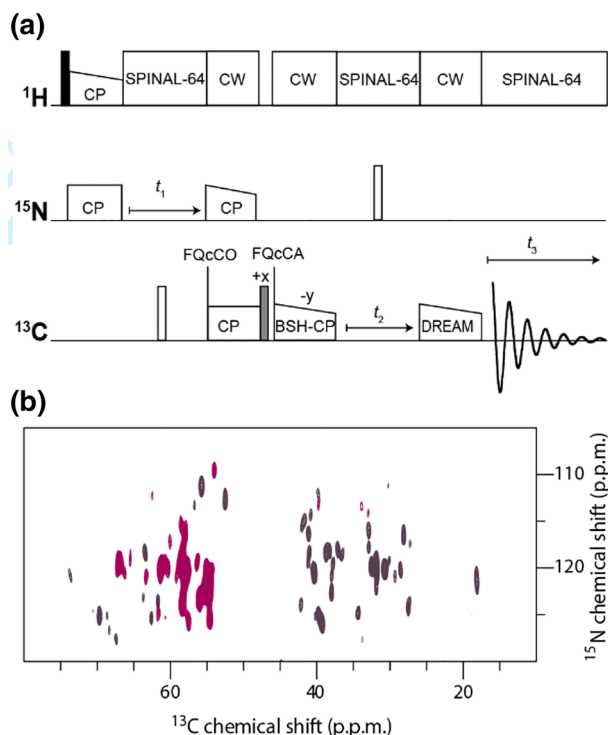
FIGURE 22 (a) Schematic representation of the 3D (H)N(CO) CACB correlation experiment pulse sequence. Filled, empty, and gray rectangles represent 90° pulses, 180° pulses, and trim pulses, respectively. (b) 3D (H)N(CO)CACB spectrum of uniformly ^{13}C–^{15}N-labeled MxiH needles (83aa) in a 3.2-mm rotor at 17.5-kHz MAS, projection along the ^{15}N–^{13}CB-plane over the whole ^{13}CA chemical shift range. Positive signals in pink represent remaining magnetization on CA nuclei, whereas negative signals in gray show CB resonances

sequence code. Optimized parameters for this experiment that can act as a guideline are listed in Table 13.

104. Use the offset parameters from Step 1 for the setup of this experiment.
105. Use all the optimized power levels, contact times, acquisition times, offset positions, and spectral widths from the (H)NCO(CA)CB experiment.

TABLE 13 Set of optimized experimental parameters for the acquisition of a 3D (H)N(CO)CACB spectrum

Parameter	Value
t_2 evolution	CA
Field (kHz)-H	82.8
180° pulse	N
Spectral width	4 kHz/23 ppm
Acquisition time (ms)	5
Detection (t_3)	C
Field (kHz)-H	82.2

106. Use CW decoupling on the proton channel during the BSH-CP and DREAM transfer. Use SPINAL-64 decoupling during acquisition.
107. Set the acquisition times to 10 ms for the direct dimension, 5 ms for the carbon indirect dimension, and 6 ms for the nitrogen indirect dimension.
108. Set the number of scans to an integer multiple of the number of phase cycle steps. Set the recycle delay to 2 s.
109. A 1D version of the (H)N(CO)CACB spectrum can serve as reference spectrum to determine the transfer efficiency if recorded with the same number of scans as the other 1D reference spectra (32 scans). For this purpose, compare the intensity of the spectrum in the CA region to the 1D (H)NCOCA spectrum.
110. Optimize the necessary acquisition times in the indirect dimensions by acquiring the 2D (H) N(CO)CACB versions of the spectrum.
111. Using the optimized parameters, acquire the 3D (H)N(CO)CACB spectrum (Figure 22b).

5 | ANTICIPATED RESULTS

The implementation of the above protocol will yield a set of one 2D and six 3D NMR spectra. The conducted experiments correlate the nuclei of the protein backbone atoms within one residue ((H)CC, (H)NCACO, and (H)NCACB) and between neighboring residues ((H)NCOCA, (H) NCO(CA)CB, (H)N(CO)CACB, and (H)CANCO) as shown schematically in Figures 23 and 24.

In the PDSD experiment, magnetization is transferred first from hydrogen nuclei to carbon nuclei from where it is transferred further on to other carbon nuclei that are close in space (Figure 23a). This results in a spectrum where practically all carbon atoms within a certain distance of one another are correlated by cross peaks (Figure 23b). Using short mixing times (≤50 ms), all carbon atoms within one residue will be correlated, whereas at longer mixing times, interresidual correlations between nuclei of neighboring amino acids will appear as well.

Some amino acids feature very characteristic side-chain carbon chemical shifts (e.g., serine or threonine) or cross-peak patterns, like isoleucine (Figure 23b). Hence, these residues are very convenient starting points regarding the backbone chemical shift assignment.

Having identified all the cross peaks belonging to one such residue i in the PDSD and thus knowing the CA$_i$ chemical shift, other resonances of this residue can be found in the 3D (H)NCACO and (H)NCACB spectra.
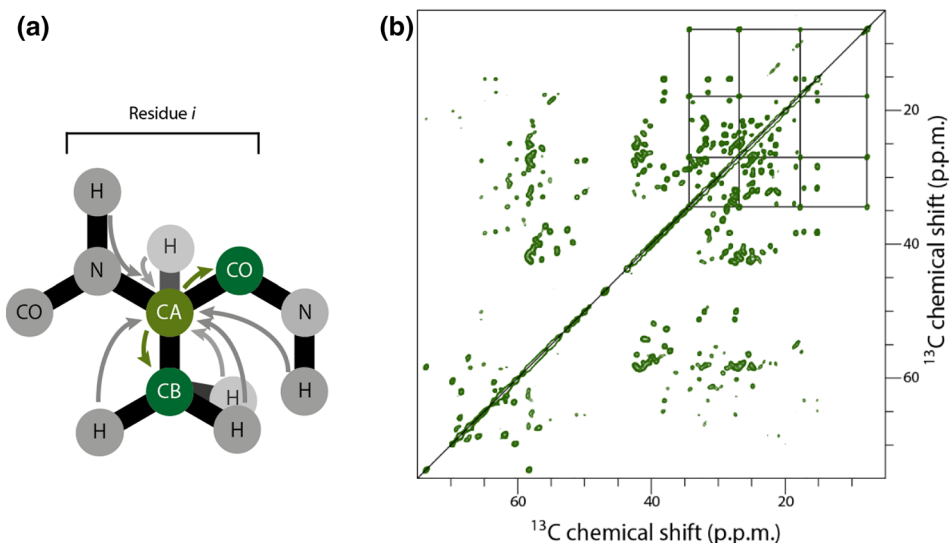
FIGURE 23 (a) Schematic representation of the magnetization transfer in the 2D (H)CC PDSD experiment described in this tutorial at the example of an alanine residue. The protein backbone of one residue (i) is indicated. Colored circles represent nuclei whose chemical shifts are acquired in the experiment. For clarity, only the transfer chain via CA as the first carbon nucleus is shown. (b) PDSD spectrum of uniformly ^{13}C–^{15}N-labeled MxiH needles (83aa) in a 3.2-mm rotor at 17.5-kHz MAS. The grid highlights side-chain cross peaks of Ile71. Because of this characteristic pattern, isoleucine residues are easy to identify in a PDSD spectrum and therefore are convenient starting points for a chemical shift assignment
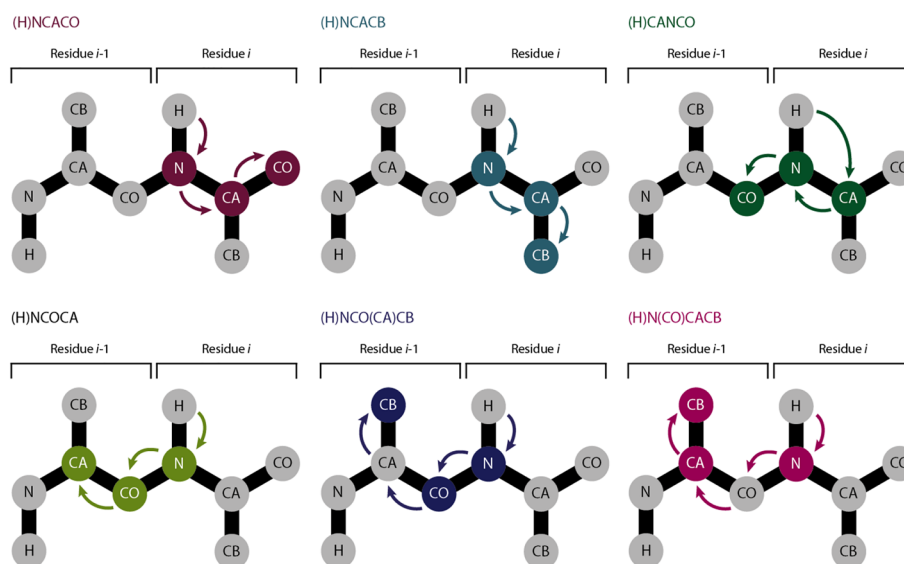

FIGURE 24 Schematic representation of the magnetization transfers in the 3D NMR experiments described in this tutorial. The protein backbone of two neighboring residues (i and $i − 1$) is indicated. Colored circles represent nuclei whose chemical shifts are acquired in the experiment

As the next step, the $CO_{i − 1}$ chemical shift of the preceding residue $i − 1$ can be identified in the (H)CANCO spectrum. With this information, the $CA_{i − 1}$ chemical shift can be detected in the (H)NCOCA spectrum, and the $CB_{i − 1}$ chemical shift can be identified in the (H)NCO(CA)CB and (H)N(CO)CACB spectra. As the last step, all the cross peaks belonging to the residue $i − 1$ can be found in the PDSD spectrum based on the already known $CA_{i − 1}$ and $CB_{i − 1}$ chemical shifts, and the amino acid type of residue $i − 1$ can be determined based on amino acid-specific average chemical shifts (Figure 24).

Ambiguities can occur here but can be solved in most cases by consulting the known primary sequence. The resonances in question have to be assumed to belong to one of the residues that come into consideration, the
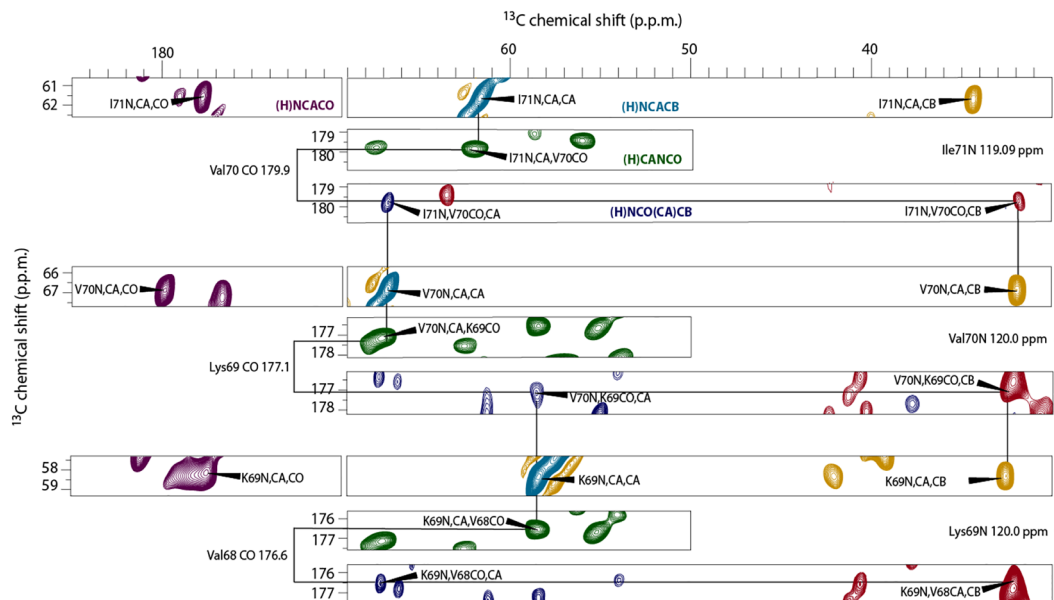
FIGURE 25 Backbone walk for chemical shift assignment using a ^{13}C–^{15}N-labeled MxiH needle protein sample (83aa) under 17.5-kHz MAS. Shown is the assignment of backbone atoms of the amino acid patch between residues Ile71 and Val68 in the form of a strip plot. The overlaid 2D spectral planes are color-coded: (H)NCACO in violet, (H)NCACB in turquoise (positive contours) and ochre (negative contours), (H)CANCO in green, (H)NCO(CA)CB in blue (positive contours), and red (negative contours). The solid lines represent the same chemical shifts and connect the peaks, establishing intraresidual and interresidual connections. All peaks used for the backbone walk are annotated with their chemical shift assignment. The chemical shift values of the z-axes defining the 2D plane positions are annotated on the right

assignment is continued, and if the following amino acid type is in accordance with the sequence, the assumption is confirmed. If this is not the case, the assumption was wrong and has to be discarded.

When all chemical shifts of the preceding residue $i - 1$ have been determined, it can become the known residue i. The procedure can be repeated for the next neighboring residue, step by step yielding a complete assignment of the protein backbone. Whenever this procedure comes to a halt, for example, because of ambiguous resonances, a new starting point needs to be chosen in order to proceed with the assignment. By inverting the procedure, the so-called "backbone walk" can be conducted in the inverse direction, identifying the next neighboring residue instead of the preceding one.

Figure 25 illustrates the steps of this backbone walk taking the example of MxiH (see Table 14 for achieved transfer efficiencies). Starting from Ile71, the individual assignment steps described above are displayed navigating through strip plots of the acquired 3D spectra. If the spectra have a good resolution, the described procedure should yield a nearly complete and unambiguous assignment of all the inflexible residues of the protein backbone as well as some atoms of the amino acid side-chains.

TABLE 14 Achieved transfer efficiencies for u-^{13}C–^{15}N-labeled MxiH needles in a 3.2-mm rotor at 17.5-kHz MAS in a 700 MHz ^{1}H Larmor frequency spectrometer

Transfer step	Transfer efficiency (%)	Reference spectrum
NCA, SPECIFIC-CP	30	(H)C$_{200\mu s}$
NCO, SPECIFIC-CP	35	(H)C$_{1ms}$
NCACO, BSH-CP	40	(H)NCO
NCOCA, BSH-CP	34	(H)NCA

CONFLICT OF INTERESTS

The authors declare no competing financial interests.

ORCID

Kitty Hendriks https://orcid.org/0000-0003-4168-1706
Adam Lange https://orcid.org/0000-0002-7534-5973

REFERENCES

[1] A. Goldbourt, *Curr. Opin. Biotechnol.* **2013**, *24*(4), 705.

[2] M. J. Knight, A. J. Pell, I. Bertini, I. C. Felli, L. Gonnelli, R. Pierattelli, T. Herrmann, L. Emsley, G. Pintacuda, *Proc. Natl. Acad. Sci.* **2012**, *109*(28), 11095.

[3] I. Sengupta, P. S. Nadaud, J. J. Helmus, C. D. Schwieters, C. P. Jaroniec, *Nat. Chem.* **2012**, *4*, 410.

[4] S. Jehle, P. Rajagopal, B. Bardiaux, S. Markovic, R. Kühne, J. R. Stout, V. A. Higman, R. E. Klevit, B. J. van Rossum, H. Oschkinat, *Nat. Struct. Mol. Biol.* **2010**, *17*, 1037.

[5] A. Loquet, N. G. Sgourakis, R. Gupta, K. Giller, D. Riedel, C. Goosmann, C. Griesinger, M. Kolbe, D. Baker, S. Becker, A. Lange, *Nature* **2012**, *486*, 276.

[6] R. Tycko, *Annu. Rev. Phys. Chem.* **2011**, *62*(1), 279.

[7] C. Wasmer, A. Lange, H. van Melckebeke, A. B. Siemer, R. Riek, B. H. Meier, *Science* **2008**, *319*(5869), 1523.

[8] M. Hong, Y. Zhang, F. Hu, *Annu. Rev. Phys. Chem.* **2012**, *63*(1), 1.

[9] S. J. Ullrich, U. A. Hellmich, S. Ullrich, C. Glaubitz, *Nat. Chem. Biol.* **2011**, *7*, 263.

[10] L. S. Brown, V. Ladizhansky, *Protein. Sci.: A Publ. Protein Soc.* **2015**, *24*(9), 1333.

[11] S. Wang, V. Ladizhansky, *Prog. Nucl. Magn. Reson. Spectrosc.* **2014**, *82*, 1.

[12] M. Hong, *J. Biomol. NMR* **1999**, *15*(1), 1.

[13] J.-P. Demers, P. Fricke, C. Shi, V. Chevelkov, A. Lange, *Prog. Nucl. Magn. Reson. Spectrosc.* **2018**, *109*, 51.

[14] P. Fricke, V. Chevelkov, M. Zinke, K. Giller, S. Becker, A. Lange, *Nat. Protoc.* **2017**, *12*, 764.

[15] M. Baldus, A. T. Petkova, J. Herzfeld, R. G. Griffin, *Mol. Phys.* **1998**, *95*(6), 1197.

[16] S. Dusold, A. Sebald, Dipolar recoupling under magic-angle spinning conditions, in *Annual Reports on NMR Spectroscopy*, Academic Press, London **2000** 185.

[17] C. R. Morcombe, V. Gaponenko, R. A. Byrd, K. W. Zilm, *J. Am. Chem. Soc.* **2004**, *126*(23), 7196.

[18] K. Takegoshi, S. Nakamura, T. Terao, *Chem. Phys. Lett.* **2001**, *344*(5), 631.

[19] I. Scholz, M. Huber, T. Manolikas, B. H. Meier, M. Ernst, *Chem. Phys. Lett.* **2008**, *460*(1), 278.

[20] R. Verel, M. Ernst, B. H. Meier, *J. Magn. Reson.* **2001**, *150*(1), 81.

[21] V. Chevelkov, K. Giller, S. Becker, A. Lange, *J. Magn. Reson.* **2013**, *230*, 205.

[22] V. Chevelkov, C. Shi, H. K. Fasshuber, S. Becker, A. Lange, *J. Biomol. NMR* **2013**, *56*(4), 303.

[23] C. Shi, H. K. Fasshuber, V. Chevelkov, S. Xiang, B. Habenstein, S. K. Vasa, S. Becker, A. Lange, *J. Biomol. NMR* **2014**, *59*(1), 15.

[24] C. Shi, Y. He, K. Hendriks, B. L. de Groot, X. Cai, C. Tian, A. Lange, H. Sun, *Nat. Commun.* **2018**, *9*(1), 717.

[25] M. Salvi, B. Schomburg, K. Giller, S. Graf, G. Unden, S. Becker, A. Lange, C. Griesinger, *Proc. Natl. Acad. Sci.* **2017**, *114*(12), 3115.

[26] M. Hora, R. Sarkar, V. Morris, K. Xue, E. Prade, E. Harding, J. Buchner, B. Reif, *PLoS ONE* **2017**, *12*(7), e0181799.

[27] S. Vasa, L. Lin, C. Shi, B. Habenstein, D. Riedel, J. Kühn, M. Thanbichler, A. Lange, *Proc. Natl. Acad. Sci.* **2015**, *112*(2), E127.

[28] L. Gremer, D. Schölzel, C. Schenk, E. Reinartz, J. Labahn, R. B. G. Ravelli, M. Tusche, C. Lopez-Iglesias, W. Hoyer, H. Heise, D. Willbold, G. F. Schröder, *Science* **2017**, *358*, 116.

[29] H. K. Fasshuber, N. A. Lakomek, B. Habenstein, A. Loquet, C. Shi, K. Giller, S. Wolff, S. Becker, A. Lange, *Protein Sci.* **2015**, *24*(5), 592.

[30] B. Habenstein, A. Loquet, S. Hwang, K. Giller, S. K. Vasa, S. Becker, M. Habeck, A. Lange, *Angew. Chem. Int. Ed.* **2015**, *54*(40), 11691.

[31] F. Ravotti, L. Sborgi, R. Cadalbert, M. Huber, A. Mazur, P. Broz, S. Hiller, B. H. Meier, A. Böckmann, *Biomol. NMR Assign.* **2016**, *10*(1), 107.

[32] D. S. Wishart, C. G. Bigam, J. Yao, F. Abildgaard, H. J. Dyson, E. Oldfield, J. L. Markley, B. D. Sykes, *J. Biomol. NMR* **1995**, *6*(2), 135.

[33] Y. T. van den Hoogen, P. P. Lankhorst, P. Gijsman, A. J. Hartel, J. H. van Boom, C. Altona, *Eur. J. Biochem.* **1988**, *171*(1-2), 143.

[34] B. M. Fung, A. K. Khitrin, K. Ermolaev, *J. Magn. Reson.* **2000**, *142*(1), 97.

[35] U. Haeberlen, J. S. Waugh, *Phys. Rev.* **1968**, *175*(2), 453.

SUPPORTING INFORMATION

Additional supporting information may be found online in the Supporting Information section at the end of the article.